ENGINEERING TREATMENT MODEL (ETM) FOR CREEP CRACK DRIVING FORCE ESTIMATION

Li Zhonghua, W. Brocks, and K.-H. Schwalbe

GKSS-Research Center, Institute for Material Research
21502 Geesthacht, Germany

ABSTRACT

Based on finite element analyses, a set of formulas for estimating the crack tip opening displacement in terms of δ_s^c in creeping materials and C^* for three fracture specimens in both plane stress and plane strain conditions are presented. Validation of these formulas has been performed for different creep laws. It has been shown that: (1) The creep δ_s^c formulas accurately match finite element results; (2) The δ_s^c is independent of the material's creep law; (3) The calculation of creep δ_s^c, and the creep fracture analysis based on δ_s^c are very convenient. They can be done by use of the nominal net section stress defined by the limit load of the cracked body and the original uniaxial creep curve at the corresponding net section stress level; (4) Due to (2) and (3) the δ_s^c is a promising parameter for creep fracture analysis; (5) Under steady-state creep and constant loading conditions, C^* is path independent for creep materials defined by $\varepsilon_c = D\sigma_n^N t^p$, and for creep strain hardening materials defined by $\dot{\varepsilon}_c = (A\sigma_n^N((m+1)\varepsilon_c)^m)^{1/(m+1)}$; (6) In the case of C^*-path independence, the provided C^*-formulas match accurately finite element results.

1. INTRODUCTION

In recent years, several procedures for the assessment of defects at high temperature have been developed [1,2,3]. These are based on evaluations of the crack tip parameters, such as stress intensity factor K, C^*-integral, or related $C(t)$ and C_t which are the generalization of C^*, and the material data describing creep crack initiation and growth. The K parameter may find application only for very creep-brittle materials and small scale creep. A number of experimental results on creep ductile materials [4,5,6] showed that the C^*-integral is an effective parameter for creep ductile materials.

The C^*-integral, upon modifying the J integral as a parameter to represent the amplitude of the stress strain field ahead of a crack tip is successful only when the material is purely viscous which corresponds to secondary, or steady state creep. C^* is subject to the same restriction as the J integral with regard to path independence. When the creep rate is defined by Norton's law

$$\dot{\varepsilon} = \alpha\sigma^N$$

the value of C^* may also be calculated from the finite element solutions tabulated in [7]. This specific stress-strain rate relation is convenient for analytical purposes, but is not a prerequisite for the validity of C^* [8]. In general cases, finite element analysis is required for obtaining C^*.

The actual situation for the creep fracture analysis is that there is not a single parameter available for the whole creep process including initial, secondary, and tertiary regimes, and no simple method to predict C^* but Norton's law.

As compared with C^*, the parameter of crack tip opening displacement (CTOD) is rarely used in creep fracture. The reason may be due to the following facts: one is the parameter being difficult to measure in practice, and the other is that there is no strictly analytical solution for predicting CTOD. To overcome these difficulties, the Engineering Treatment Model (ETM) was developed for piece-wise power law materials [9,10]. In the ETM, a special definition of CTOD was used, which measures the CTOD at the specimen's side surface, spanning the original

crack tip over a gauge length of 5 mm, and which is therefore termed δ_5. This definition is numerically close to values determined after BS576 [11]. A set of simple formulas for estimating δ_5 and J integral are also provided. Extensive validation of the ETM has been performed so far on laboratory specimens [9,10] and fracture analyses of structural parts [12,13]. Recently, under deformation theory of plasticity and monotonic loading conditions the ETM has been extended to pure power law as well as non-power law materials, and therefore proved that the ETM-concept is valid over a wide range of materials [14].

The CTOD parameter is less restrictive than the J or C^* integrals. Following the ETM-concept, the two inherent shortcomings mentioned above may be overcome. The CTOD in terms of δ_5 may become a promising load parameter for the fracture analysis in a wide range of creep behavior.

In this paper, the ETM formulas are developed based on finite element analyses in order to obtain approximate but accurate estimates of the CTOD in terms of δ_5^c in creeping conditions and C^* for three fracture specimens. Validation of these formulas has been performed for different creep laws. All the calculations are carried out using the ABAQUS code.

2. CREEP ETM FOR CTOD IN TERMS OF δ_5^c

2.1 Creep Deformation Behavior Described by δ_5^c.

Based on a large number of creep FE-analysis on three test specimens, the creep deformation behavior described by δ_5^c as a function of nominal net section strain, ε_c, as shown in Fig. 1, can be summarized as follows:

(1) After initial non-linear response, δ_5^c is a linear function of the nominal net section creep strain ε_c. The slope of the straight line is independent of the net section stress, σ_n, for a given crack length (Fig. 1(a)), but is strongly crack length dependent (Fig. 1(b)).

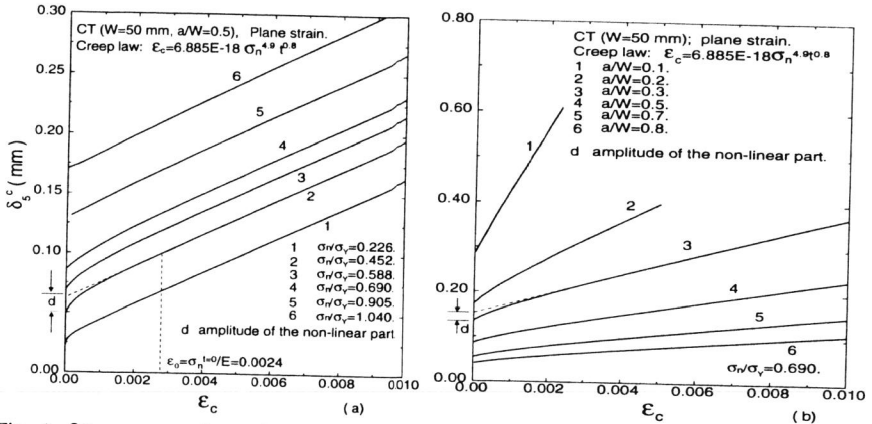

Fig. 1 $\delta_5^c - \varepsilon_c$ curves for a CT specimen at different stress levels (a) and for a CT specimen with different crack lengths at the same stress level calculated by FE-analysis. (yield stress σ_Y=515 MPa, elastic modulus E=97000 MPa for a Titanium alloy).

(2) The initial non-linear part in the δ_5^c versus ε_c disappears when $\varepsilon_c = \varepsilon_0$ ($\varepsilon_0 = \sigma_n^{t=0}/E$ defined as initial strain, see Fig. 1(a)). The amplitude of the non-linear part is stress (Fig. 1(a)) and crack length (Fig. 1(b)) dependent. When the applied nominal net section stress $\sigma_n = \sigma_Y$ (σ_Y is the yield stress), the non-linear part of the $\delta_5^c - \varepsilon_c$ curve vanishes altogether.

The above creep deformation behaviors correspond to two creep deformation stages, namely: transition creep and widespread creep stages. In the transition creep stage, the deformation behavior is controlled by elastic and creep strains and the crack tip undergoes stress redistribution and blunting. In the widespread creep stage, δ_5^c as a linear function of the net section creep strain gives an unequivocal description of the steady-state creep.

The requirement for the stress redistribution to be complete and the widespread creep conditions to be established may be expressed in terms of a transition time t_{red}. From the FE-results, t_{red} can be determined in terms of

$$\varepsilon_c(\sigma_n, t_{red}) = \varepsilon_0. \tag{1}$$

This is in agreement with the definition proposed by Ainsworth [15].

2.2 Formulas for Predicting Creep δ_5^c.

Based on the observations summarized in the above section, creep δ_5^c can be expressed as:

$$\delta_5^c = \delta_{5_0} + \delta_{5C} \tag{2-1}$$

$$\delta_{5C} = \delta_{5C\,\text{linear}} + \delta_{5C\,\text{non-linear}} \tag{2-2}$$

$$\delta_{5C\,\text{linear}} = (W-a)\beta(\lambda)\varepsilon_c \tag{2-3}$$

$$\delta_{5C\,\text{non-linear}} = (W-a)\eta_1(\lambda)\eta_2(\alpha)(1-\exp(-4\varepsilon_c/\varepsilon_0)) \quad \text{for } \varepsilon_0 < \varepsilon_Y \tag{2-4}$$

$$\delta_{5C\,\text{non-linear}} = 0 \quad \text{for } \varepsilon_0 \geq \varepsilon_Y \tag{2-5}$$

where the subscripts 0 and C denote the initial value at the start of creep deformation and the value due to creeping, respectively. δ_{5_0} can be estimated by the elastic-plastic ETM [9]. In the present study, it is calculated by FE-analysis in order to check the accuracy of predicting of δ_{5C} (Eq. (2-2)). The nominal net section creep strain, ε_c, is determined from the creep law at nominal net section stress. To formulate Eq. (2), a general form of the creep law is used by

$$\varepsilon_c = D\sigma_n^N t^p, \tag{3}$$

in which D, N and p are material constants. In Eq. (2) ε_0 is the nominal net section initial strain, i.e. at $t = 0$, defined by

$$\varepsilon_0 = \sigma_n^{t=0}/E \tag{4}$$

and

$$\varepsilon_Y = \sigma_Y/E \tag{5}$$

is the nominal net section yield strain at which $\sigma_n = \sigma_Y$, and E is the Young's modulus.

In Eqs. (3) and (4), the nominal net section stress, σ_n, is defined by

$$\sigma_n = F\sigma_Y/F_Y \tag{6}$$

where F and F_Y are the generalized applied load and limit load, respectively. The formulas of F_Y for the specimens used are given in appendix A.

The normalized factors $\beta(\lambda)$ and $\eta_1(\lambda)$ in Eq. (2) are functions of normalized crack length, $\lambda = a/W$ (a is crack length, W is the width of the specimen), and the factor $\eta_2(\alpha)$ is a function of the normalized stress, $\alpha = \sigma_n/\sigma_Y$. Based on finite element analyses, they can be expressed as:

For Three Point Bend (TPB) specimens,

$$\beta(\lambda) = 0.9081 - 1.4776\lambda + 1.2518\lambda^2 \tag{7-1}$$

$$\eta_1(\lambda) = 0.0052 + 0.0192\lambda + 0.0429\lambda^2 - 0.0479\lambda^3 \tag{7-2}$$

$$\eta_2(\alpha) = 0.0001 + 0.122\alpha - 0.0317\alpha^2 - 0.0904\alpha^3 \tag{7-3}$$

for plane stress, and

$$\beta(\lambda) = 0.309 + 0.0295\lambda - 0.0247\lambda^2 + 0.209\lambda^3 \tag{8-1}$$

$$\eta_1(\lambda) = 0.0231 + 0.0564\lambda - 0.2161\lambda^2 + 0.1859\lambda^3 \tag{8-2}$$

$$\eta_2(\alpha) = 0.0732\alpha - 0.0454\alpha^2 - 0.0279\alpha^3 \tag{8-3}$$

for plane strain.

For the Compact Tension (CT) specimens

$$\beta(\lambda) = 2.41 - 10.73\lambda + 24.38\lambda^2 - 24.91\lambda^3 + 9.68\lambda^4 \quad (9\text{-}1)$$

$$\eta_1(\lambda) = 0.0213 - 0.1646\lambda + 1.1503\lambda^2 - 2.0759\lambda^3 + 1.1439\lambda^4 \quad (9\text{-}2)$$

$$\eta_2(\alpha) = 0.001 + 0.104\alpha - 0.105\alpha^2 \quad (9\text{-}3)$$

for plane stress, and

$$\beta(\lambda) = 5.61 - 40.08\lambda + 113.15\lambda^2 - 136.29\lambda^3 + 59.64\lambda^4 \quad (10\text{-}1)$$

$$\eta_1(\lambda) = 0.0156 + 0.2452\lambda - 0.6863\lambda^2 + 0.5955\lambda^3 \quad (10\text{-}2)$$

$$\eta_2(\alpha) = -0.0167 + 0.161\alpha - 0.258\alpha^2 + 0.113\alpha^3 \quad (10\text{-}3)$$

for plane strain.

For the Center Cracked Tension (CCT) specimens,

$$\beta(\lambda) = 0.1965 + 2.7054\lambda - 4.7647\lambda^2 + 3.1948\lambda^3 \quad (11\text{-}1)$$

$$\eta_1(\lambda) = 0.0045 + 0.0110\lambda + 0.0402\lambda^2 \quad (11\text{-}2)$$

$$\eta_2(\alpha) = -0.0321 + 0.344\alpha - 0.515\alpha^2 + 0.203\alpha^3 \quad (11\text{-}3)$$

for plane stress, and

$$\beta(\lambda) = 0.0714 + 1.1296\lambda - 2.0075\lambda^2 + 1.3728\lambda^3 \quad (12\text{-}1)$$

$$\eta_1(\lambda) = 0.0078 + 0.0418\lambda - 0.1148\lambda^2 + 0.158\lambda^3 \quad (12\text{-}2)$$

$$\eta_2(\alpha) = -0.0083 + 0.1424\alpha - 0.128\alpha^2 \quad (12\text{-}3)$$

for plane strain.

2.3 Basic Characters and applications of δ_s^c-ETM.

As examples, comparisons between the δ_s^c predicted by Eq. (2) and FE-analyses are given in Fig. 2(a) for a CT specimen at different stress levels in plane stress condition, and in Fig. 2(b) for CT specimens with different crack lengths in plane strain condition. As shown in Fig. 2, Eq. (2) can accurately replicate FE-results. Similar agreement is found for TPB and CCT specimens.

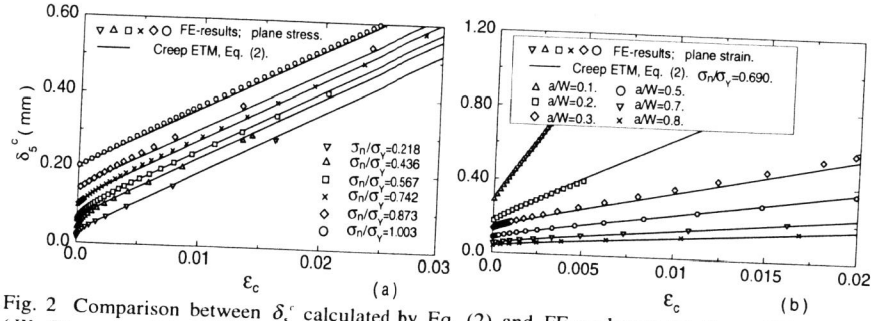

Fig. 2 Comparison between δ_s^c calculated by Eq. (2) and FE-analyses: (a) for a CT specimen (W=50 mm, a/W=0.5) at different stress levels, and (b) for CT specimens (W=50 mm) with different crack lengths.

Because δ_{sc} in Eq. (2) is only net section creep strain dependent for a given geometry and applied load, it should be independent of the creep law parameters. This is true as shown in Fig. 3(a) for differing stress index N, and in Fig. 3(b) for varying time index, p, of the creep law defined by Eq. (3).

Based on the same argument, Eq. (2) is creep law independent as shown in Fig. 4(a) for the creep law defined by

$$\dot{\varepsilon}_c = A(\sinh(\sigma_n/\sigma_Y))^N \quad (13)$$

and in Fig. 4(b) for a creep strain hardening material defined by

$$\dot{\varepsilon}_c = \left\{A\sigma_n^N[(m+1)\varepsilon_c]^m\right\}^{\frac{1}{m+1}} \quad (14)$$

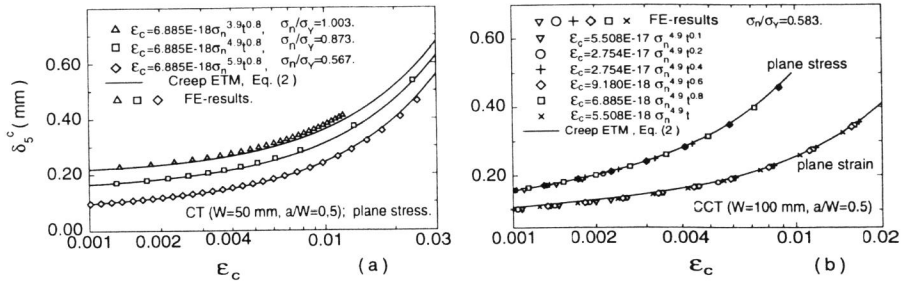

Fig. 3 δ_s^c-ETM is valid for changing stress index N (a), and for changing time index P (b) in the creep law of Eq. (3).

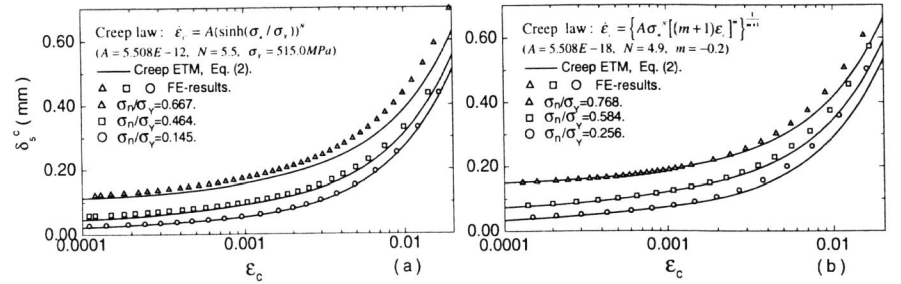

Fig. 4 δ_s^c-ETM formula (Eq. (2)) is also valid for different creep laws.

3. CREEP ETM FOR THE C^*-INTEGRAL

3.1 Formulas for Predicting C^*.

The C^*-integral, defined in analogy to the J-integral, was introduced by Landes and Begley [16]:

$$C^* = \int_\Gamma (W^* dy - T_i \frac{\partial \dot{u}_i}{\partial x} ds) \quad (15)$$

with the components T_i of traction vector on an integration path Γ, $\dot{u}_i$ the components of the displacement rate vector, the stress work rate W^* is given by

$$W^* = \int_0^t \sigma_{ij} d\dot{\varepsilon}_{ij} \quad (16)$$

C^* is path-independent for the same reasons that the J-integral is path-independent in nonlinear elastic materials.

By analogy with J calculation, the C^* parameter may be expressed as [17]

$$C^* = \sigma_n \dot{\varepsilon}_c(\sigma_n) L(a, \lambda, \varepsilon_c) \quad (17\text{-}1)$$

where $\dot{\varepsilon}_c$ is the creep strain rate at the net section stress, and $L(a, \lambda, \varepsilon_c)$ is a geometry and creep strain dependent characteristic length, and can be written as

$$L(a, \lambda, \varepsilon_c) = (W - a)\xi_1(\lambda)\xi_2(\varepsilon_c) \quad (17\text{-}2)$$

Based on finite element analyses, $\xi_1(\lambda)$ and $\xi_2(\varepsilon_c)$ can be expressed as:
For TPB specimens

$$\xi_1(\lambda) = 1.2671 + 0.1029\lambda - 9.5354\lambda^2 + 18.8657\lambda^3 - 10.3815\lambda^4 \quad (18\text{-}1)$$
$$\xi_2(\varepsilon_c) = 35779.0\exp(-(\varepsilon_c + 0.016898)/0.001618) + 0.9887 \quad (18\text{-}2)$$

for plane stress, and

$$\xi_1(\lambda) = 0.5345 + 0.9883\lambda - 0.5584\lambda^2 + 0.0170\lambda^3 \quad (19\text{-}1)$$
$$\xi_2(\varepsilon_c) = 27287.0\exp(-(\varepsilon_c + 0.018192)/0.001766) + 0.9764 \quad (19\text{-}2)$$

for plane strain.
For CT specimens

$$\xi_1(\lambda) = 3.7649 - 15.1730\lambda + 29.6039\lambda^2 - 25.9812\lambda^3 + 8.5422\lambda^4 \quad (20\text{-}1)$$
$$\xi_2(\varepsilon_c) = 158120.0\exp(-(\varepsilon_c + 0.045658)/0.00363) + 0.9536 \quad (20\text{-}2)$$

for plane stress, and

$$\xi_1(\lambda) = 21.55 - 134.10\lambda + 337.49\lambda^2 - 375.69\lambda^3 + 154.58\lambda^4 \quad (21\text{-}1)$$
$$\xi_2(\varepsilon_c) = 29.9656 * \exp(-(\varepsilon_c + 0.010158)/0.002631) + 0.9687 \quad (21\text{-}2)$$

for plane strain.
For CCT specimens

$$\xi_1(\lambda) = 0.1828 + 3.8467\lambda - 6.4236\lambda^2 + 3.5724\lambda^3 \quad (22\text{-}1)$$
$$\xi_2(\varepsilon_c) = 607410.0\exp(-(\varepsilon_c + 0.020928)/0.001532) + 0.9891 \quad (22\text{-}2)$$

for plane stress, and

$$\xi_1(\lambda) = 0.077931 + 1.870\lambda - 3.0305\lambda^2 + 1.6945\lambda^3 \quad (23\text{-}1)$$
$$\xi_2(\varepsilon_c) = 64.4501\exp(-(\varepsilon_c + 0.011063)/0.002659) + 0.9497 \quad (23\text{-}2)$$

for plane strain.

3.2 Basic Properties and Applications of C^*-ETM.

As examples, comparisons between the C^* predicted by Eq. (17) and FE-analyses are given in Fig. 5(a) for a CCT specimen at different stress levels in plane stress condition, and in Fig. 5(b) for CCT specimens withdifferent crack lengths in plane strain condition. As shown in Fig. 5, Eq. (17) can accurately replicate FE-results. Similar coincidence is found for TPB and CT specimens.

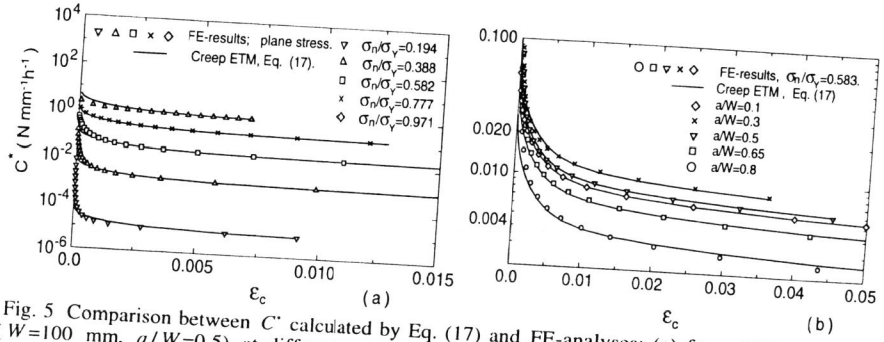

Fig. 5 Comparison between C^* calculated by Eq. (17) and FE-analyses: (a) for a CCT specimen (W=100 mm, a/W=0.5) at different stress levels in plane stress condition, and (b) for CCT specimens (W=50 mm) with different crack lengths in plane strain condition. (creep law: $\dot{\varepsilon}_c = 6.885E-18\sigma_n^{4.9}t^{0.8}$).

Because C^* in Eq. (17) is net section creep strain and its rate dependent for a given geometry and applied load, it is valid for changing stress index, N, of the creep law (Eq. 3) as shown in Fig. 6(a), and for changing time index, p, as shown in Fig. 6(b).

Figure 7(a) shows that for creep strain hardening material C^* is path independent, and the C^*-ETM formula (Eq. (17)) is valid.

For creeping materials in which C^* is path dependent, C^*-ETM formula gives a similar prediction as one of these path as shown in Fig. 7(b).

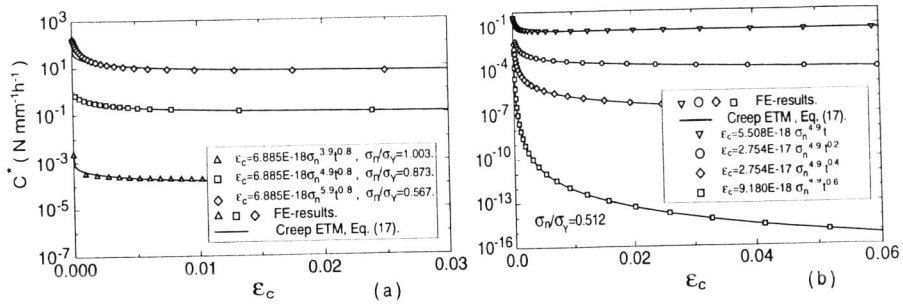

Fig. 6 Comparisons between C^* calculated by Eq. (17) and FE-analyses: (a) for a CT specimen (W=50 mm, a/W=0.5, plane stress) with different stress index N in Eq. (3), and (b) for TPB specimens (W=100 mm, a/W=0.5, plane strain) with different time index p in Eq. (3).

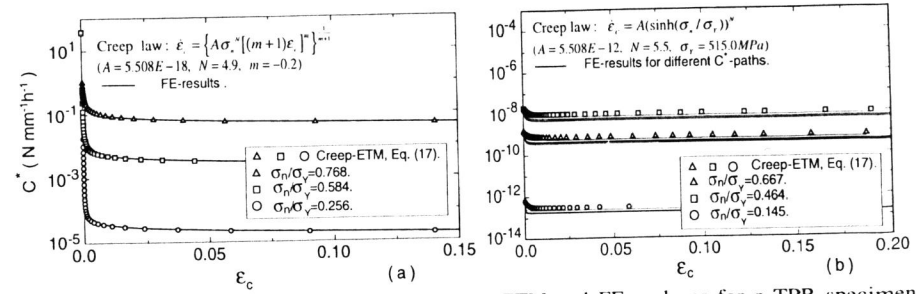

Fig. 7 Comparisons between C^* predicted by creep ETM and FE-analyses for a TPB specimen (W=100 mm, a/W=0.5, plane stress): (a) for a creep strain hardening material, and (b) for creeping materials in which C^* is path dependent.

4. CONCLUSIONS AND DISCUSSION

(1) When the net section creep strain is larger than the initial net section strain, a steady-state creep condition is reached. δ_s^c as a linear function of the net section creep strain gives an unequivocal description of the steady-state creep.

(2) The creep δ_s^c-ETM formula is independent of the creep law of the material, creep law parameters, and therefore can be used in the whole creep process including initial, secondary, and tertiary creep regimes.

(3) For a stationary creep crack, the creep δ_s^c-ETM formulas accurately replicates finite element results.

(4) The calculation of creep δ_s^c is very convenient. The only parameter required for the calculation is the limit load of the cracked body. Because creep δ_s^c is creep law independent, a closed form of the creep law is not necessary for practice, and the creep strain needed for the calculation can be directly determined on the original uniaxial creep curve at the corresponding net section stress level.

(5) The creep fracture analysis based on creep δ_s^c is sensible and convenient. From the critical δ_s^c values of creep crack incubation and creep crack rupture, the corresponding critical creep strains can be determined by Eq. (2). The creep crack incubation time t_i and creep crack rupture time t_r can be determined from the given creep law or directly determined on the uniaxial creep curve at the corresponding net section stress level.

(6) Under steady-state creep condition defined by Eq. (1), finite element analyses show that under constant loading condition C^* is path independent for the creeping materials defined by Eq. (3) and for creep strain hardening materials.

(7) In the case of C^*-path independence, C^*-ETM formula accurately replicate finite element results.

(8) As compared with δ_s^c, C^* is subject to more restrictions for engineering applications.

REFERENCES

1. R. A. Ainsworth, G. G. Chell, M. C. Coleman, W. Goodall, D. J. Gooch, J. R. Haigh, S. T. Kimmins, and G. J. Neate: Fatigure Fract. Engng. Matr. Struct., **10**(1987), 115-127.
2. R5: Procedure for High Temperature Response of Structures, Nuclear Electric Report R5 Issue 1, Berkeley Technology Center (1990).
3. P. Piques, E. Molinie and A. Pineau: Fatigure Fract. Engng. Matr. Struct. **14**(1987), 871-885.
4. E. Mass, P. Piques: Engng Fract. Mech., **22**(1985), 307-325.
6. A. Saxena: ASTM STP **700**(1980), 131-157.
7. V. Kumar, M. D. German, and C. F. Shih: An Engineering Approach for Elastic-Plastic Analysis, EPRI Report NP-1931, Palo Alto(1981).
5. D. J. Smith and G. A. Webster: J. Strain Anyl., **16**(1981), 137-143.
8. H. Riedel: ICF-7, Houston, Texas, March 1989.
9. K.-H. Schwalbe and A. Cornec: Fatigue Fract. Engng Mater. Struct. **14**(1991), 405-412
10. K.-H. Schwalbe: GKSS **84/E/38**(1984), GKSS-Research Center, Geesthacht GmbH.
11. K.-H. Schwalbe: The Crack Tip Opening Displacement in Elastic-Plastic Fracture Mechanics, Springer-Verlag, Heidelberg, 1985, F. R. Germany, 133-156.
12. K.-H. Schwalbe and L. Grüter: Engng Fract. Mech., **42**(1992), 221-235.
13. S. Hao, A. Cornec and K.-H. Schwalbe: Journal of Pressure Vessel Technology, **115**(1993), 164-170.
14. Li Zhonghua, W. Brocks and K.-H. Schwalbe: Fatigue Fract. Engng Mater. Struct., to be published.
15. R. A. Ainsworth: Int. J. Solids Structure, **18**(1982), 873-881.
16. J. D. Landes and J. A. Begley: ASTM STP **590**(1976), 128-140.
17. R. A. Ainsworth: Int. J. Fracture, **20**(1982), 147-159.

Appendix A

For the limit load the following formulas were used:
For Compact Tension specimens,

$$F_Y = \eta_p \sigma_Y BW \tag{A1-1}$$

with

$$\eta_p = \sqrt{2.155*(1.0+1.155(a/W)^2)} - 1 - 1.155a/W \tag{A1-2}$$

for plane stress, and

$$\eta_p = 1.155(\sqrt{2.7+4.59(a/W)^2} - 1.0 - 1.7a/W) \tag{A1-3}$$

for plane strain.
For Three Point Bend specimens,

$$F_Y = \eta_p \sigma_Y BW^2(1-a/W)^2/S \tag{A2}$$

with $\eta_p = 1.072$ for plane stress, and $\eta_p = 1.455$ for plane strain.
For Center Cracked Tension specimens,

$$F_Y = 2\sigma_y(1-a/W)BW \tag{A3}$$

for both plane stress and strain conditions.